Clinical Cancer Research

Myeloid-Derived Suppressor Cell Subset Accumulation in Renal Cell Carcinoma Parenchyma Is Associated with Intratumoral Expression of IL1β, IL8, CXCL5, and Mip-1α

Yana G. Najjar[1], Patricia Rayman[2], Xuefei Jia[3], Paul G. Pavicic Jr[2], Brian I. Rini[4], Charles Tannenbaum[2], Jennifer Ko[5], Samuel Haywood[6], Peter Cohen[7], Thomas Hamilton[2], C. Marcela Diaz-Montero[2], and James Finke[2]

Abstract

Purpose: Little is known about the association between myeloid-derived suppressor cell (MDSC) subsets and various chemokines in patients with renal cell carcinoma (RCC) or the factors that draw MDSC into tumor parenchyma.

Experimental Design: We analyzed polymorphonuclear MDSC (PMN-MDSC), monocytic MDSC (M-MDSC), and immature MDSC (I-MDSC) from the parenchyma and peripheral blood of 48 patients with RCC, isolated at nephrectomy. We analyzed levels of IL1β, IL8, CXCL5, Mip-1α, MCP-1, and Rantes. Furthermore, we performed experiments in a Renca murine model to assess therapeutic synergy between CXCR2 and anti-PD1 and to elucidate the impact of IL1β blockade on MDSC.

Results: Parenchymal PMN-MDSC have a positive correlation with IL1β, IL8, CXCL5, and Mip-1α, and I-MDSC correlate with IL8 and CXCL5. Furthermore, peripheral PMN-MDSC correlate with tumor grade. Given that PMN-MDSC express CXCR2 and parenchymal PMN-MDSC correlated with IL8 and CXCL5, we assessed the response of CXCR2 blockade with or without anti-PD1. Combination therapy reduced tumor weight and enhanced $CD4^+$ and $CD8^+$ T-cell infiltration. In addition, anti-IL1β decreased PMN-MDSC and M-MDSC in the periphery, PMN-MDSC in the tumor, and peripheral CXCL5 and KC. Anti-IL1β also delayed tumor growth.

Conclusions: Parenchymal PMN-MDSC have a positive correlation with IL1β, IL8, CXCL5, and Mip-1α, suggesting they may attract PMN-MDSC into the tumor. Peripheral PMN-MDSC correlate with tumor grade, suggesting prognostic significance. Anti-CXCR2 and anti-PD1 synergized to reduce tumor weight and enhanced $CD4^+$ and $CD8^+$ T-cell infiltration in a Renca murine model, suggesting that $CXCR2^+$ PMN-MDSC are important in reducing activity of anti-PD1 antibody. Finally, anti-IL1β decreases MDSC and delayed tumor growth, suggesting a potential target for MDSC inhibition. *Clin Cancer Res; 23(9); 2346–55. ©2016 AACR.*

Introduction

Renal cell carcinoma (RCC) accounted for 3.8% of newly diagnosed cancers in the United States in 2014, with close to 64,000 new cases diagnosed (SEER data), which indicates a consistent increase in the incidence rate since 1975 (1). The discovery that biallelic loss of the von Hippel Lindau (VHL) tumor suppressor gene results in increased transcription of growth factors involved in RCC tumorigenesis has resulted in a major paradigm shift in the landscape of RCC treatment, with the development and subsequent approval of several targeted therapies (2). It is well established that tumor-mediated immunosuppression of the microenvironment and immunoevasion contribute to decreased clinical efficacy of immune and targeted therapy (3–5). Along with checkpoint blockade of T-cell function (6), multiple cell types are involved in tumor-mediated immunosuppression, including type 2 natural killer T (NKT) cells, tumor-associated macrophages (TAM), regulatory T cells (Treg), and myeloid-derived suppressor cells (MDSC; refs. 7, 8). MDSC are a heterogeneous cell population that is thought to play a major role in tumor-mediated immunoevasion; they arise from myeloid progenitor cells that fail to differentiate into mature dendritic cells, granulocytes, or macrophages and are distinguished by the capacity to suppress T-cell and NK cell function (8, 9). That MDSC use several mechanisms to suppress antitumor immunity has been demonstrated both *in vitro* and *in vivo*. These mechanisms include cysteine sequestration to decrease proliferation, activation, and differentiation of T cells (8), depletion of L-arginine to arrest T cells in mitosis (10), induction of $FoxP3^+$ Treg cells (11), downregulation of CD4 and CD8 T-cell homing to lymph nodes, and conversion of antitumor M1 cells into tumor-promoting M2 cells (12). MDSC also promote the tumor vasculature via their production of different angiogenic proteins (13, 14). MDSC in

[1]Department of Hematology-Oncology, University of Pittsburgh Cancer Institite, Pittsburgh, Pennsylvania. [2]Department of Immunology, Cleveland Clinic Foundation, Cleveland, Ohio. [3]Department of Quantitative Health Sciences, Cleveland Clinic Foundation, Cleveland, Ohio. [4]Cleveland Clinic Foundation, Taussig Cancer Center, Cleveland, Ohio. [5]Pathology Institute, Cleveland Clinic, Cleveland, Ohio. [6]Department of Urology, Cleveland Clinic Foundation, Cleveland, Ohio. [7]Division of Hematology-Oncology, Mayo Clinic, Scottsdale, Arizona.

Corresponding Author: C. Marcela Diaz-Montero, Department of Immunology, Lerner Research Institute, Cleveland Clinic, 9500 Euclid Avenue, Cleveland, OH 44195. Phone: 216-445-7697; Fax: 216-444-9329; E-mail: diazc2@ccf.org

doi: 10.1158/1078-0432.CCR-15-1823

Translational Relevance

We show that total myeloid-derived suppressor cell (MDSC), polymorphonuclear (PMN-MDSC), and immature MDSC (I-MDSC) in the periphery of patients with renal cell carcinoma (RCC) are increased compared with normal controls and that PMN-MDSC correlate with grade, which if validated in a larger cohort, could represent a prognostic marker. Furthermore, we show that parenchymal PMN-MDSC have a positive correlation with IL8, CXCL5, Mip-1α, and IL1β and I- MDSC correlate positively with IL8 and CXCL5. We also show that in a Renca murine model, treatment with CXCR2 antagonist increased $CD4^+$ and $CD8^+$ T-cell infiltration and enhanced the efficacy of anti-PD1 antibody, an important finding in the era of checkpoint inhibitors. Furthermore, IL1β blockade resulted in decreased parenchymal PMN-MDSC, peripheral PMN, and monocytic MDSC (M-MDSC) and decreased tumor progression. This suggests that anti-IL1β may be a potential strategy to target immune inhibitory MDSC. These findings warrant further investigation as methods of enhancing the efficacy of immunotherapy in patients with RCC.

humans are broadly characterized as expressing $CD33^+$, $CD11b^+$, and HLA-$DR^{low/-}$, and multiple MDSC populations have been described in patients with solid tumors. Polymorphonuclear MDSC (PMN-MDSC) additionally express CD15 and are CD14-negative, whereas monocytic MDSC (M-MDSC) express CD14 and not CD15. Immature MDSC (I-MDSC) express neither CD14 nor CD15 (8, 15).

Peripheral MDSC levels are significantly increased in patients with cancer and correlate with metastatic burden, clinical cancer stage, and outcome. In a study of 106 patients with solid malignancies (although this did not include patients with RCC), circulating MDSC correlated with clinic stage and tumor burden (16). While PMN-MDSC, M-MDSC, and I-MDSC have been described in patients with RCC, PMN-MDSC are the dominant population in peripheral blood of many different types of cancer, including RCC (17, 18). A recent study identified 6 MDSC phenotypes in patients with RCC, 5 of which were increased in the periphery compared with healthy donors; the monocytic and PMN-MDSC subtypes correlated with overall survival (19). Indeed, of all the described MDSC subsets, only 3 have been shown to correlate with clinical outcomes in patients with cancer (20). Two studies (one in gastrointestinal cancers and one in breast cancer) have shown that increasing levels of $CD33^+$HLA-DR^-CD11b^+MDSC in the periphery correlate with decreased overall survival (OS; refs. 21, 22). M-MDSC levels have also been shown to inversely correlate with OS (19) and have been described as an independent risk factor for recurrence in hepatocellular carcinoma (23). M-MDSC frequency has also been correlated with median progression-free survival (PFS) in non–small cell lung cancer (24). PMN-MDSC have been associated with decreased OS time in gastric cancer (24) and in RCC (19). All of the aforementioned studies pertained only to peripheral MDSC; to our knowledge, no correlation has been made between intratumoral MDSC levels and recurrence-free survival (RFS).

MDSC are induced by chronic inflammation, and inflammatory factors, such as IL6 (25), IL1β (26, 27), GM-CSF (28), S100A8/S9A, and prostaglandin E2 (29), have been shown to promote MDSC accumulation. While associations have been shown between MDSC and various chemokines in the periphery of murine and human cancer hosts, little is known about the factors that draw MDSC directly into the tumor parenchyma, including human RCC.

The chemokine receptor CXCR2 is a key mediator of neutrophil migration (30, 31), and its ligands, IL8 and CXCL5, have been shown to be chemoattractants for PMN-MDSC (32–37). CXCR2 is known to be an important chemokine receptor that directs the recruitment of tumor promoting leukocytes into tissue and the inhibition of this receptor significantly suppresses inflammation-driven and spontaneous tumorigenesis (38, 39). In established murine tumors, blocking of CXCR2 using $cxcr2^{-/-}$ mice or by treating with cxcr2 antibodies/antagonists promotes tumor regression and enhances anti-PD1 efficacy of blockade-mediated immunotherapy (32, 40). Mip-1α is a ligand of CCR5, which is known to be involved in acute inflammation and recruitment and activation of neutrophils (33–35). Finally, MCP-1 is a ligand of CCR2, which is known to recruit $CD11bGr1^+$ MDSC into tumors (41). Little is known about factors that draw I-MDSC into human tumor parenchyma. In addition, it is known that IL1β induces inflammation, leading to the production of chemoattractants for MDSC, including PMN-MDSC, such as IL8 (42).

Here, we analyzed the relationship between circulating or intratumoral levels of MDSCs and tumor grade, stage, and RFS in patients with RCC. In addition, we determined whether a correlation exists between these parenchymal/peripheral blood MDSC subsets and levels of IL1β, IL8, CXCL5, Mip-1α, MCP-1, and Rantes in the parenchyma and peripheral blood in patients with primary RCC tumors, before patients receiving any treatment, to elucidate some of the factors that might promote MDSC accumulation, particularly the PMN-MDSC subset, as it is the largest population in patients with RCC. In addition, the expression of the chemokine receptor CXCR2 on human and mouse PMN-MDSC was examined along with testing the possibility that $CXCR2^+$ myeloid cells promote tumor growth

Materials and Methods

Tumor lysates

Primary RCC tumor samples were collected from 48 patients prior to nephrectomy, in accordance with an institutional IRB-approved protocol. Samples were divided and a portion of the tumor was flash-frozen to make lysates using the Fastprep-24 (MP Biomedicals) according to the manufacturer's manual. Briefly, tumor tissue was placed in Lysing Matrix D tubes with RIPA Buffer (Thermo Scientific) and protease inhibitor (Sigma) and Halt Phosphatase inhibitors (Thermo Scientific), incubated and processed in the FastPrep-24. The lysates were then aliquoted and frozen at −80°C.

Phenotype analysis of MDSC subsets from tumor

Phenotyping of MDSC was performed on fresh tumor samples. Using flow cytometry, we phenotyped PMN-MDSC, M-MDSC, and I-MDSC from the parenchyma of 48 RCC nephrectomy samples (Fig. 1, with MDSC subsets expressed as means). Tumor was digested by first cutting tissue into small fragments followed

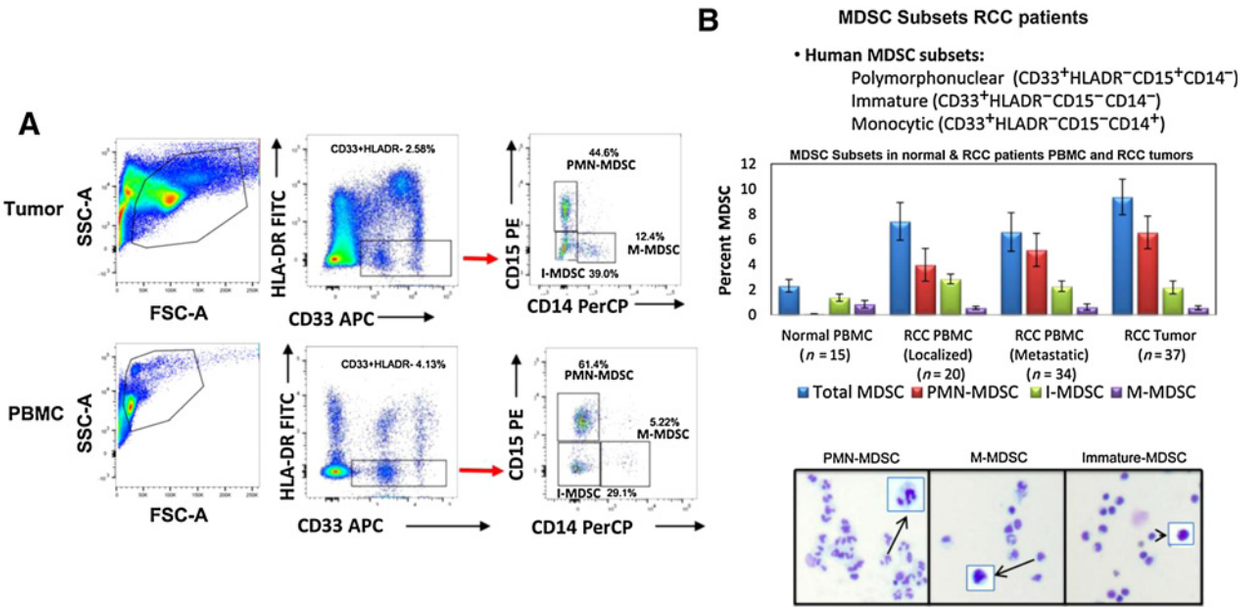

Figure 1.

A, Representative flow cytometric graphics for RCC tumor and PBMC showing the gating scheme and subsets. **B,** Percentage of MDSC subsets from normal individuals and PBMCs from both localized and patients with metastatic RCC and tumors. Compared with healthy donors, the percentage of MDSC, particularly the PMN and linage-negative subsets are significantly increased in the peripheral blood and tumor of patients with RCC. The morphology of the MDSC subsets is also shown. The MDSC subsets were sorted from an RCC tumor; cytospins were made and stained with Diff-Quik Stain Set. The insets show cells at 2×.

by incubation (15 minutes) with enzyme cocktail [Collagenase 1 mg/mL (Sigma), 0.1 mg/mL DNase (Sigma), and 2.5 U/mL hyaluronidase (Sigma)] and then filtered using 70-μm cell strainers (BD Falcon). Thereafter, the single-cell suspension was subjected to 30% percoll gradient over a 70% percoll gradient to enrich for mononuclear cells and to remove debris, followed by staining cells with anti-CD33 APC, anti-HLA-DR FITC, anti-CD15 PE, and anti-CD14 PerCP antibodies, along with appropriate isotype controls (all from BD) for flow cytometry acquisition (BD FACSCalibur), and analysis (CellQuest Pro, BD). Total MDSC were defined as $CD33^+$ $HLA\text{-}DR^{low/-}$; PMN-MDSC were defined as $CD33^+$ $HLA\text{-}DR^{low/-}$ $CD14^-CD15^+$; M-MDSC were defined as $CD33^+$ $HLA\text{-}DR^{low/-}$ $CD14^+$ $CD15^-$, and I-MDSC were defined as $CD33^+$ $HLA\text{-}DR^{low/-}$ $CD14^-$ $CD15^-$. Some tumors were further stained with CD66b (BD) and CXCR2 (R&D Systems) antibodies. CD66b [also known as carcinoembryonic antigen–related cell adhesion molecule 8 (CEACAM8)] is expressed primarily on granulocytes and granulocytic MDSC (36, 37). CXCR2 is a member of the CXC chemokine receptor family binding several chemokines such as IL8 that are involved in inflammation and is strongly associated with neutrophil attraction (43).

To assess the morphology of MDSC in RCC tumors, MDSC preparation from the percoll gradient was stained with markers for MDSC (CD33, HLA-DR, CD15, and CD14), and individual subsets were then isolated by high-speed cell sorting (Aria FACS). Cytospins were made and then stained with Diff-Quik staining solution.

Phenotype analysis of MDSC subsets from peripheral blood

Peripheral blood was obtained prior to surgery from 22 of the 48 patients from whom we had tumor samples, in addition to 33 patients with metastatic disease for whom we did not have tumor tissue. Fifteen controls were available from healthy donors. All samples were obtained in accordance with our IRB protocol. Patient blood was subjected to Ficoll Hypaque density centrifugation, and the buffy layer containing peripheral blood mononuclear cells, including MDSC, was stained with the same antibodies as the tumor for flow cytometric analysis (see above).

The FACS data are presented as the percentage of MDSC subsets in the peripheral blood mononuclear cell (PBMC) buffy layer following Ficoll Hypaque density centrifugation. The percentage of MDSC subsets in the tumor is calculated from the single-cell suspension after digestion of tumor and percoll gradient centrifugation.

Chemokine and IL1β levels from tumor and peripheral blood

ELISA (R&D Systems) was used to quantitate levels of IL1β, IL8, CXCL5, Mip-1α, MCP-1, and Rantes in tumor lysates. Plasma was available from 20 of the 48 patients from whom we had tumor samples, and 15 healthy controls. ELISA (R&D systems) was used to measure levels of IL1β, IL8, CXCL5, Mip-1α, MCP-1, and Rantes in plasma. A protein assay (Pierce BCA Protein Assay, Thermo Scientific) was done on both parenchymal and peripheral blood samples to ensure equal amounts of protein were aliquoted in each well. Manufacturer instructions were followed for the ELISA.

Mouse experiments

Renca cells (1×10^6) were injected subcutaneously into Balb/c mice. After 14 days, tumor-bearing mice were treated for 21 days with CXCR2 antagonist (40 μg/mouse, once daily intraperitoneally), anti-PD1 antibody (200 μg/mouse, 2 times per week), or the

combination. Anti-IL1β treatment (100 μg/mouse, 2 times a week) started 10 days after tumor implantation and lasted 3 weeks. CXCR2 antagonist was purchased from Tocris Bioscience. Anti-PD1 and anti-IL1β antibodies were purchased from Bioexcell. Untreated Renca tumor–bearing mice served as controls. The tumors were harvested, weighed, and digested with enzyme cocktail Collagenase (1 mg/mL, Sigma), DNase (0.1 mg/mL, Sigma), and hyaluronidase (2.5 U/mL, Sigma) and then filtered using 70-μm cell strainers (BD Falcon). The single-cell suspensions were stained with CD4 (eBioscience), CD8, Ly6G, CD11b (all from BD Bioscience), and CXCR2 (R&D Systems) antibodies. The cells were acquired for flow cytometry using a BD FACSCalibur and analysis was done using FlowJo (Treestar).

Statistical methods

Categorical variables were summarized as frequency counts and percentages, measured data as medians and ranges. The Wilcoxon rank-sum and Jonckheere–Terpstra tests were used for the comparison of MDSC between patient groups. Spearman rank correlations were used to assess the association between MDSC and inflammatory factors in tumor samples and blood from patients with RCC. Time to recurrence was measured from the date of nephrectomy to the date of progression on imaging or last follow-up and was analyzed using proportional hazards models. All *P* values are 2-tailed and performed at a significance level of 0.05. SAS 9.3 software (SAS Institute) was used for all analyses.

Results

Patient characteristics

The present cohort included 48 patients with RCC prior to nephrectomy. Median age was 62.9 years (range: 39–82.8) and 34 patients (70.8%) were male. All included patients (100%) had clear cell carcinoma. Ten patients (20.8%) had grade 2 histology, 28 (58.3%) had grade 3, and 10 (20.8%) grade 4 histology. Twenty-six patients (54.2%) had stage I–II, 15 (31.3%) had stage 3, and 7 patients (14.6%) had metastatic (stage IV) disease at the time of nephrectomy (Table 1). Of the 7 patients with metastases, 7 had lung, lymph node, or adrenal involvement, 3 had liver metastases, and 1 each had bone or stomach metastases. Peripheral blood was available from 22 of the 48 patients, and blood was available from 33 patients who did not have tumor samples available. No patient had received any systemic anticancer treatment prior to nephrectomy. The peripheral blood analysis of MDSC subsets in patients with RCC was compared to the same populations in the PBMC fraction from healthy controls.

Table 1. Patient characteristics

Factor	All tumor (*N* = 49)	Tumor and blood (*N* = 22)	All blood (*N* = 55)
Age, y	62.8 (36.0–82.8)	—	—
Tumor			
Total MDSC	6.1 (0.42–37.0)	8.9 (1.1–30.3)	—
M-MDSC	0.25 (0.00–4.9)	0.18 (0.00–1.9)	—
I-MDSC	1.1 (0.05–15.6)	1.6 (0.10–15.6)	—
PMN-MDSC	3.0 (0.00–31.2)	6.2 (0.50–28.9)	—
Blood			
Total MDSC	—	5.1 (2.3–25.4)	3.5 (0.31–47.1)
M-MDSC	—	0.42 (0.01–2.8)	0.40 (0.00–4.1)
I-MDSC	—	2.0 (0.68–6.8)	2.0 (0.20–7.9)
PMN-MDSC	—	1.7 (0.05–21.2)	1.9 (0.05–38.0)
Gender			
Female	15 (30.6)	8 (36.4)	15 (27.3)
Male	34 (69.4)	14 (63.6)	40 (72.7)
Grade			
2	10 (20.8)	7 (31.8)	11 (25.6)
3	28 (58.3)	12 (54.5)	20 (46.5)
4	10 (20.8)	3 (13.6)	12 (27.9)
Stage			
1	24 (50.0)	12 (54.5)	12 (21.8)
2	2 (4.2)	1 (4.5)	1 (1.8)
3	15 (31.3)	6 (27.3)	6 (10.9)
4	7 (14.6)	3 (13.6)	36 (65.5)

MDSC subset levels are increased in the peripheral blood and tumor of patients with RCC relative to MDSC levels detected in the blood from normal healthy donors

Figure 1A shows the gating strategy and analysis of the 3 major MDSC subsets based on staining for CD33, HLA-DR, CD15, and CD14. Compared with healthy donor PBMC ($n = 15$), the numbers of PMN-MDSC and I-MDSC are significantly increased in the blood and tumor (Fig. 1B). The morphology of the 3 subsets is also shown.

Peripheral blood was available from 55 patients and 15 normal controls (Table 2, with MDSC subsets expressed as medians). Comparing MDSC subset levels in each cohort, we found that total MDSC are 3.5% in patients versus 1.8% in controls (a 1.94-fold increase, $P = 0.002$). In addition, PMN-MDSC were 47.5-fold elevated in patients with RCC compared with controls (1.9% vs. 0.04%, respectively; $P < 0.001$). I-MDSC were also elevated in patients compared with controls (2.0% vs. 1.09%, a 1.83-fold increase; $P = 0.003$). Levels of M-MDSC did not differ significantly between the 2 cohorts. Furthermore, levels of MDSC did not differ when comparing limited stage (stage I, II, and III) to patients with stage IV disease.

Peripheral blood PMN-MDSC levels correlate with tumor grade

In our analysis, increasing peripheral levels of PMN-MDSC correlate with higher tumor grade ($P = 0.006$). As with M-MDSC levels in patients versus controls, we did not find a correlation between peripheral M-MDSC levels and tumor grade, nor did we find a correlation between peripheral levels of total MDSC or I-MDSC and grade. Parenchymal levels of MDSC subsets did not correlate with tumor grade. No MDSC subset in the peripheral blood correlated with tumor stage.

Peripheral MDSC subset data and RFS data were available from 16 patients with stage I to III disease. Likewise, tumor samples were available from 34 patients with limited stage (stage I–III) disease. We used 48 patients for immune analysis but 8 of those have limited follow-up time, so we excluded them from the RFS analysis. The tumor PMN-MDSC population was found to be marginally significant for RFS ($P = 0.0505$). With our current sample size, other MDSC subsets in the tumor did not correlate with RFS, nor did peripheral MDSC correlate with RFS.

Table 2. Comparison of MDSC subsets in blood between patients with cancer and normal controls

Factor	Normal (*N* = 15)	Patients (*N* = 55)	*P*
Total MDSC	1.8 (0.49–7.5)	3.5 (0.31–47.1)	0.002
M-MDSC	0.41 (0.00–3.4)	0.40 (0.00–4.1)	0.86
I-MDSC	1.09 (0.31–4.1)	2.0 (0.20–7.9)	0.003
PMN-MDSC	0.04 (0.01–0.23)	1.9 (0.05–38.0)	<0.001

Table 3. Correlation between MDSC and IL8, IL1, CXCL5, MIP-1α, MCP-1, and RANTES in tumor and blood samples from patients with RCC

	Chemokines					
Tumor lysate	**IL8 (*P*)**	**CXCL5 (*P*)**	**Mip-1α (*P*)**	**MCP-1 (*P*)**	**RANTES (*P*)**	**IL1β (*P*)**
Total MDSC	<0.001	<0.001	0.01	0.96	0.45	0.02
PMN-MDSC	<0.001	<0.001	0.014	0.8	0.64	0.029
M-MDSC	0.13	0.058	0.57	0.64	0.28	0.97
I-MDSC	0.033	0.008	0.63	0.98	0.68	0.14
Total blood	**IL8**	**CXCL5**	**Mip-1α**	**MCP-1**	**RANTES**	**IL1β**
Total MDSC	0.82	0.61	0.47	0.10	0.32	0.003
PMN-MDSC	0.50	0.54	0.32	0.15	0.79	0.067
M-MDSC	0.41	0.67	0.49	0.87	0.68	0.82
I-MDSC	0.41	0.87	0.19	0.32	0.45	0.21

NOTE: The coefficients for the correlations for the tumor with $P < 0.05$ range from 0.34 to 0.65 and for blood are 0.6 and 0.4, respectively.

MDSC subsets correlate with certain chemokines and IL1β

We examined RCC tumor tissue for expression of chemokines known to promote the trafficking of PMN-MDSC and neutrophils (IL8, CXCL5, and Mip-1α; refs. 32–35). MCP1 levels were examined, as it is known to cause MDSC accumulation in a mouse tumor model (41). We also examined the expression of IL1β in the tumors, as this inflammatory cytokine is known to induce the production of chemokines like IL8 and CXCL5, thereby indirectly promoting MDSC recruitment (44).

Here, we show that parenchymal levels of PMN-MDSC have a positive correlation with IL8 ($P < 0.001$), CXCL5 ($P < 0.001$), and Mip-1α ($P = 0.014$; Table 3). Intratumor levels of IL1β ($P = 0.029$) also correlated with PMN-MDSC levels in tumor tissue. Rantes (CCL5) levels did not correlate with MDSC accumulation. In addition, we show that levels of I-MDSC correlate positively with IL8 ($P = 0.033$) and CXCL5 ($P = 0.008$), but not IL1β (Table 3).

The analysis of blood MDSC, chemokines, and IL1β levels revealed that total MDSC correlated with IL1β plasma levels ($P = 0.003$) and that PMN-MDSC levels trended toward correlation which did not reach statistical significance (Table 3). Blood M-MDSC and I-MDSC subsets did not correlate with any of the chemokines or interleukins we analyzed (Table 3). We did not find any significant differences between levels of IL1β, IL8, CXCL5, Mip-1α, MCP-1, and Rantes in the blood of patients versus normal controls (data not shown).

Treatment of mice bearing Renca tumors with CXCR2 antagonist enhanced the efficacy of anti-PD1 therapy

Because intratumor levels of PMN-MDSC ($CD33^+HLA\text{-}DR^-CD15^+CD14^-$) correlated with intratumor levels of IL8 and CXCL5, we tested these cells for their expression of CXCR2 which binds IL8 and CXCL5 and is a prominent chemokine receptor expressed on neutrophils and PMN-MDSC (Fig. 2D). Analysis of 15 localized patients with RCC demonstrated that 50% of the intratumoral PMN-MDSC expressed CXCR2. Further analysis showed that PMN-MDSC from 10 patients showed greater than 47% expression (47%–100%), one patient had 27% expression, whereas only 4 patients displayed low expression (<10%). The analysis of intratumor PMN-MDSC ($Ly6G^+CD11b^+$) in mice bearing the renal tumor cell line RENCA demonstrated that approximately 20% to 25% expressed CXCR2, which is somewhat less than the value expressed by human PMN-MDSC (Fig. 2). None of the $Ly6G^-CD11b^+$ monocytic MDSC expressed CXCR2. Because some PMN-MDSC express the chemokine receptor CXCR2, we wanted to test whether antagonizing CXCR2 would reduce tumor growth and simultaneously enhance T-cell response in the tumor. As part of this experiment, we also tested whether combining treatment using the CXCR2 antagonist with anti-PD1 antibody would improve outcome. Similar to others (32), treatment of tumor-bearing mice with anti-PD1 antibody once tumors are well established only affords modest protection (Fig. 2). However, treating RENCA-bearing mice with a CXCR2 antagonist along with anti-PD1 antibody improved the efficacy of the checkpoint blockade antibody($P \leq 0.05$; Fig. 2A), whereas treatment with the antagonist alone had minimal impact on tumor weight. Interestingly, CXCR2 antagonist alone or when combined with anti-PD1 antibody did not reduce the number of PMN-MDSC in the tumor, suggesting that the antagonist may block the suppressive function of the MDSC. However, combination treatment did increase the infiltration of both $CD4^+$ T cells ($P = 0.009$) and $CD8^+$ T cells ($P = 0.058$), which coincided with a reduction in tumor weight.

IL1β blockade inhibits PMN-MDSC recruitment and delays tumor progression

IL1β is a master regulator of chemokine/cytokine expression (45) and is known to promote MDSC accumulation in the periphery; however, less is known on its impact on intratumoral MDSCs (42). Given our data with RCC cancer patient samples that showed a correlation between MDSC levels in the tumor and the concentration of intratumoral IL1β along with select chemokines (IL8 and CXCL5), we used the Renca tumor model to test whether blocking IL1β activity would impact MDSC subset levels, concentration of select chemokines, and tumor growth. Anti-IL1β blocking antibody treatment caused a dramatic reduction in PMN-MDSC and M-MDSC in the peripheral blood ($P = 3.46E\text{-}05$ and 0.0002, respectively); however, only the PMN-MDSC subset was significantly reduced in the tumor ($P = 0.010$; Fig. 3A). ELISA of serum levels of KC, the homolog for human IL8 and CXCL5 (LIX), showed elevated concentrations of both chemokines in sera of Renca-bearing mice compared with sera from non–tumor-bearing mice. In addition, anti-IL1β treatment significantly reduced levels of both chemokines (Fig. 3B) that corresponded to the reduction in PMN-MDSC, in both the blood and tumor (Fig. 3A). Moreover, this relative short-term treatment with anti-IL1β antibody also caused a significant reduction in total tumor cellularity (Fig. 3).

Discussion

In this study, we compared MDSC subset levels in the peripheral blood of 55 patients with RCC versus 15 controls. We found that total MDSC are elevated in patients versus controls, as are PMN-MDSC and I-MDSC. These findings support those of several other groups (19, 21, 22). Levels of M-MDSC did not differ

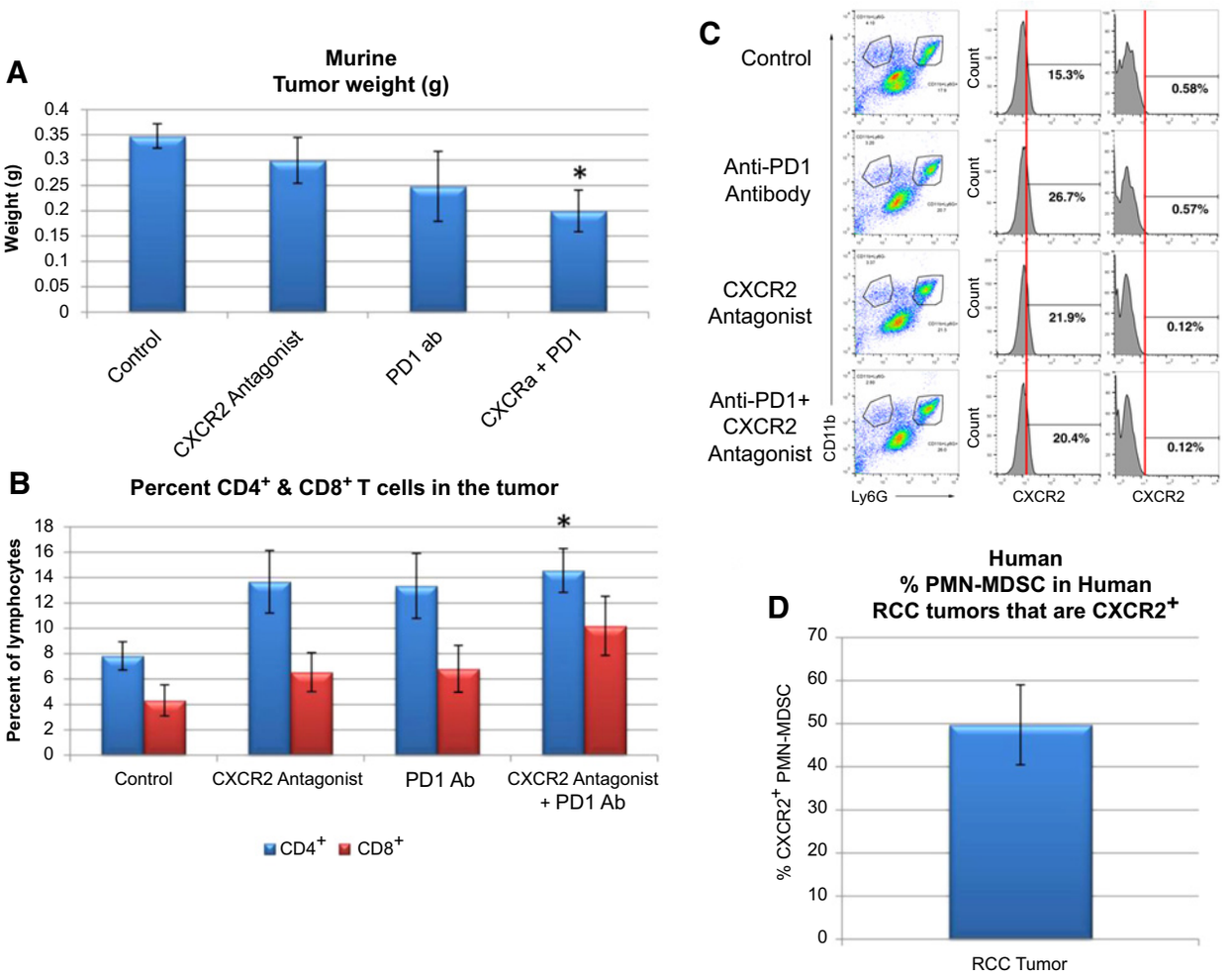

Figure 2.

A, Renca tumor–bearing mice were treated for 21 days with CXCR2 antagonist (40 μg/100 μL, once daily intraperitoneally), anti-PD1 antibody (200 μg/mouse, 2 times per week), or the combination. Untreated Renca tumor–bearing mice served as controls. The tumors were harvested and weighed. **B,** Tumors were digested; the resulting single-cell suspensions were stained with CD4 and CD8 antibodies and acquired for flow cytometry. The results show an increase in $CD4^+$ and $CD8^+$ T cells in the tumors of the treated mice, with a significant ($P = 0.02$) increase of $CD4^+$ cells with the combination treatment. **C,** Tumor single-cell suspensions were also stained for Ly6G, CD11b, and CXCR2. There was no significant change in the PMN ($CD11b^+Ly6G^+$) or monocytic ($CD11b^+Ly6G^-$) MDSC with treatment. CXCR2 was present on the PMN-MDSC but not the monocytic MDSC. **D,** Human RCC tumors were digested; the resulting single-cell suspensions were stained for CD66b, CXCR2 or CD15, HLA-DR, CD33, and CXCR2. The graph shows the mean ± SEM (median, 51.1%; range, 0.83%–100%) of PMN-MDSC that are $CXCR2^+$ in the tumor.

significantly between our 2 cohorts, likely due to M-MDSC being the lowest subset proportion. Other possible reasons for this include M-MDSC having potentially differentiated into PMN-MDSC (46) or TAM (47), or because sample size was too small. It is important to note, however, that increased peripheral blood M-MDSC levels have been shown in patients with cancer compared with controls in several other studies. Arihara and colleagues showed that M-MDSC are increased in patients with hepatocellular carcinoma (23), Huang and colleagues demonstrated that in non–small cell lung cancer, M-MDSC frequency correlates with median PFS (24), and Walter and colleagues demonstrated that M-MDSC are associated with decreased OS in RCC (19).

PMN-MDSC in the periphery of patients with RCC also correlated with increasing tumor grade. While several studies have shown a correlation between peripheral MDSC levels and patient outcomes, to our knowledge, ours is the first to show a correlation between MDSC subset levels and tumor grade in RCC. We did not find a correlation between parenchymal MDSC levels and grade, which may be due to inherent variability within the parenchyma. Small tissue samples are unlikely to be representative of the entire tumor.

In this study, we sought to assess whether parenchymal levels of MDSC correlate with RFS. Tumor samples were available from 34 patients with limited stage (stage I–III) disease. PMN-MDSC marginally correlated with RFS in patients with limited stage disease ($P = 0.0505$). Total MDSC, M-MDSC, and I-MDSC did not significantly correlate with RFS in limited stage disease, this may be because our sample size was too small to detect a significant difference (17), or because of wide variability in the immune infiltrate within the tumor. To the best of our knowledge,

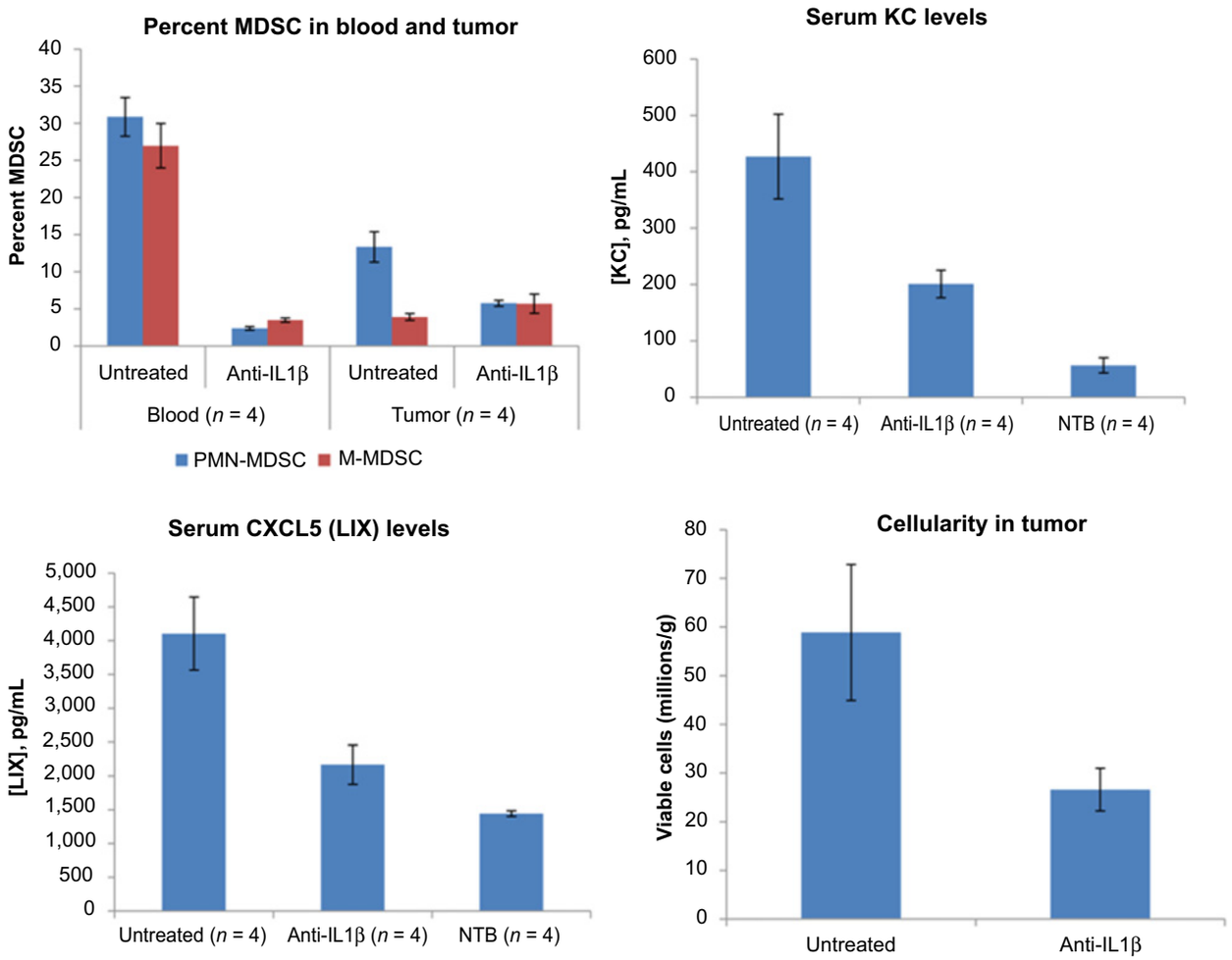

Figure 3.

A, Renca tumor–bearing mice were treated for 3 weeks with anti-IL1β (100 μg/mouse, 2 times per week). Untreated Renca tumor–bearing mice and non–tumor-bearing mice (NTB) served as controls. At harvest, blood was obtained by cardiac puncture. The tumors were digested using Miltenyi Mouse Tumor Dissociation Kit. Total number of viable cells was quantified. The single-cell suspensions from tumor digest and whole blood were stained with Ly6G and CD11b and acquired for flow cytometry. Anti-IL1β significantly reduced both the PMN-MDSC and M-MDSC in the blood ($P = 0.000035$ and $P = 0.00033$, respectively) and only the PMN-MDSC in the tumor ($P = 0.011$). **B** and **C,** ELISA were done on the serum from mice for both KC and CXCL5 (LIX). **D,** Cellularity (millions of viable cells in the tumor suspension/gram of tumor) decreased in the anti-IL1β–treated mice.

only two published studies have explored the clinical significance of intratumoral MDSCs (20, 48). In this study, Cui and colleagues demonstrated that patients whose ovarian cancer samples were $CD33^+$ high (by immunohistochemical staining) had decreased OS compared with patients with $CD33^+$ low samples (48).

PMN-MDSC derived from the peripheral blood of patients with RCC have been shown to suppress T-cell production of IFNγ and T-cell proliferation during *in vitro* coculture experiments, whereas neutrophils from healthy donors are not suppressive (Ko and colleagues, manuscript in preparation). The mechanism of suppression by PMN-MDSC is partly dependent on the arginase pathway (10, 17, 18, 49). We found that PMN-MDSC, but not healthy donor neutrophils, are angiogenic, as demonstrated by their capacity to enhance tumor blood vessel formation following co-injection with an RCC cell line (ACHN) in a xenograft model using NOD/scid mice (Ko and colleagues, manuscript in preparation). Thus, these findings support the idea that PMN-MDSC have the potential to block the development of an effective antitumor immunity, thereby promoting tumor progression. Additional support for this concept comes from a study by Highfill and colleagues showing that PMN-MDSC ($Ly6G^+CD11b^+$) promote immune suppression and can reduce the effectiveness of anti-PD1 antibody therapy in mice bearing a rhabdomyosarcoma. The reduction of PMN-MDSC with anti-CXCR2 antibody treatment decreased tumor growth and significantly improved the *in vivo* activity of anti-PD1 treatment, suggesting that preventing the trafficking of PMN-MDSC into tumors may enhance the efficacy of anti-PD1 therapy (32). Here, we show in the Renca model that an antagonist for CXCR2 when combined with anti-PD1 antibody therapy synergized to reduce tumor weight and enhance the infiltration of $CD4^+$ and $CD8^+$ T cells. We speculate that while the CXCR2 antagonist did not reduce PMN-MDSC numbers in the tumor, it may have impacted their function, a possibility we are currently testing. These findings further support

the idea that $CXCR2^+$ PMN-MDSC are important in reducing the antitumor activity of anti-PD1 antibody and promoting tumor progression.

A major focus of this study is to assess whether parenchymal levels of MDSC subsets correlate with certain chemokines and ILβ. Indeed, we found that PMN-MDSC correlated with intratumor levels of IL1β, IL8, CXCL5, and Mip-1α. These data suggest that these chemokines and IL1β promote accumulation of PMN-MDSC in the parenchyma of the RCC host. CXCR2, the receptor for IL8 and CXCL5, was expressed in more than 50% of PMN-MDSC. Although the data are associative, they suggest that this MDSC subset is drawn into the RCC tumor parenchyma by these cytokines in the tumor milieu. Indeed, CXCL5 and IL8 have been shown to be chemokines to PMN-MDSC (38).

Rantes (CCL5) did not correlate with MDSC accumulation, which was not a surprising finding given that it is primarily chemotactic for eosinophils and basophils (50). Furthermore, levels of I-MDSC correlated with IL8 and CXCL5, but not IL1β. In peripheral blood, the only significant association was between total MDSC and IL1β, although there was a trend toward an association between blood levels of IL1β and blood-derived PMN-MDSC (Table 3).Thus, in blood and tumor, IL1 levels correlated with MDSC levels. Other blood MDSC subsets did not correlate with any of the chemokines or interleukins we analyzed, and this may be a function of sample size; we were unable to detect significant differences between chemokine and IL1β between blood levels in patients and normal controls (data not shown). Other potential causes could include sample stability, as samples were frozen. Some of the normal controls may have had comorbidities or subclinical viral infections that could have caused elevations in chemokines. The pivotal role of IL1β in regulating the mobilization and recruitment of PMN-MDSCs was further corroborated by our studies using a blocking antibody. Decreases in the levels of PMN-MDSCs in both periphery and tumor correlated with reduced levels of CXCL5 and IL8 and a reduction in total tumor cellularity in the Renca model. Similarly, a recent study showed that in a prostate cancer model, a CXCR2 antagonist reduced tumor weight and prolonged survival, and anti-CXCL5 Ab or CXCR2 inhibitor reduced MDSC migration *in vitro*. In a colon cancer murine model, mice with increased levels of IL8 had increased immature myeloid cells (51).

The chemokine receptor CXCR2 is a key mediator of neutrophil migration. Its ligands, IL8 and CXCL5, have been shown to be chemoattractants for PMN-MDSC (32, 38). IL8 is a proinflammatory chemokine that is thought to promote neutrophil chemotaxis and degranulation, and increased expression of IL8 and/or its receptors has been shown in cancer cells, endothelial cells, and TAMs, suggesting it may play a significant role in the regulation of the tumor microenvironment (52).

Indeed, IL8, in addition to IL6 and TNFα, has been shown to be significantly increased in RCC tissue and its expression dependent on the degree of malignancy (53). Furthermore, higher levels of IL8 have been associated with decreased survival (9 vs. 17 months, $P = 0.0371$; ref. 53), and IL8 has been shown to be an independent predictor of OS (54). Here, we show that parenchymal levels of IL8 correlate with increased total MDSC ($P < 0.001$), PMN-MDSC ($P < 0.001$), and I-MDSC ($P = 0.033$). While these data are associative, it again suggests that IL8 plays an important role in immunomodulation of the tumor microenvironment. We found a similar association between parenchymal levels of CXCL5 and increased total MDSC ($P < 0.001$), PMN-MDSC ($P < 0.001$), and I-MDSC ($P = 0.008$), which was not surprising, given that CXCL5 and IL8 are both ligands of CXCR2, and we show that PMN-MDSC in RCC tissue express this chemokine receptor. The correlation of I-MDSC with IL8 and CXCL5 is especially interesting, given that little is known about the factors that draw I-MDSC into the tumor parenchyma. Interestingly, CXCL5 expression has been associated with decreased survival in a number of human tumors (55), and IL8 levels were recently shown to correlate with PFS and OS in mRCC (ref. 54; for CXCL5, these were studies on tumor parenchyma, whereas with IL8 this was a study on circulating protein).

Other chemokine receptors such as CCR5 likely play a role in trafficking and activation of MDSC infiltrating RCC. Indeed, we found that parenchymal levels of total MDSC and PMN-MDSC correlated with levels of Mip-1α, suggesting that perhaps PMN-MDSC or a subpopulation of these cells express CCR5 in addition to CXCR2. FACS analysis of murine PMN-MDSC derived from CT26 IL1β–expressing tumors showed dual expression of CXCR2 and CCR5 on a subset of PMN-MDSC (Tannenbaum, manuscript in preparation). It is well established that IL1β induces production of chemoattractants for PMN-MDSC, such as IL8, and we found a positive correlation between total intratumor levels of MDSC, PMN-MDSC, and IL1β.

While we did not find increased levels of chemokines or IL1β in the blood of patients compared with controls (perhaps due to our small sample size), increased IL8 has been described in the serum of patients with RCC compared with controls (56–58), and IL8 has repeatedly been linked to sunitinib resistance (59, 60). Similarly, high serum concentrations of IL1β and MCP-1 have been described in larger cohorts of patients with RCC (57), and IL1β levels have been shown to be an independent risk factor for increased risk of recurrence and decreased overall survival in limited stage RCC (61).

Our study has several limitations; our small sample size may have led to type II error in some instances, such as the inability to discern associations between peripheral/parenchymal M-MDSC and grade, stage, or RFS, or the difference between chemokine levels in the serum of patients versus controls. Furthermore, although MDSC in tumor were quantitated with freshly isolated tumor tissue, a few of the samples used for chemokine analysis had been frozen whole, then thawed, which may have led to intersample variability. Despite these limitations, our results clearly indicate that PMN-MDSC and I-MDSC are significantly increased in the blood and tumor of RCC patients, and that peripheral blood PMN-MDSC, correlate with tumor grade. Finally, we show that parenchymal levels of PMN-MDSC have a positive correlation with intratumor levels of IL1β, IL8, CXCL5, and Mip-1α, suggesting that these chemokines may attract PMN-MDSC and I-MDSC into the parenchyma of the RCC host. The increased intratumoral expression of the CXCR2 ligands (IL8 and CXCL5), the CCR5 ligand Mip-1α, along with the inflammatory cytokine IL1β likely promote the accumulation of PMN-MDSC and I- MDSC into RCC tissue, and their presence in the tumor likely promotes T-cell–mediated suppression and tumor angiogenesis.

Conclusion

Our study provides potential new targets for the risk stratification of patients with limited stage renal carcinoma, in addition

to elucidating a possible association between MDSC subsets and chemokine-induced migration into the tumor tissue. Although chemokine recruitment of PMN-MDSC had been previously suggested, little is known about the recruitment of I-MDSC and their suppressive/angiogenic activity. Targeting CXCR2, CCR5, and their ligands as well as IL1β may reduce MDSC number and function, which could enhance the efficacy of immunotherapy and targeted therapy approaches, including immune checkpoint blockade, in patients with RCC. Further research is required in larger cohorts.

Disclosure of Potential Conflicts of Interest

No potential conflicts of interest were disclosed.

Authors' Contributions

Conception and design: Y.G. Najjar, B.I. Rini, C. Tannenbaum, J. Ko, J. Finke
Development of methodology: Y.G. Najjar, B.I. Rini, J. Ko, C.M. Diaz-Montero
Acquisition of data (provided animals, acquired and managed patients, provided facilities, etc.): Y.G. Najjar, P. Rayman, P.G. Pavicic, B.I. Rini, C. Tannenbaum, S. Haywood
Analysis and interpretation of data (e.g., statistical analysis, biostatistics, computational analysis): Y.G. Najjar, X. Jia, P.G. Pavicic, B.I. Rini, C. Tannenbaum, C.M. Diaz-Montero, J. Finke
Writing, review, and/or revision of the manuscript: Y.G. Najjar, C.S. Tannenbaum, J. Ko, P Cohen, T. Hamilton, C.M. Diaz-Montero, J. Finke
Administrative, technical, or material support (i.e., reporting or organizing data, constructing databases): Y.G. Najjar
Study supervision: Y.G. Najjar, B.I. Rini, C. Tannenbaum, T. Hamilton, J. Finke

Grant Support

The study was supported by RO1CA168488 and RO1CA150959 grants and by Pfizer.

The costs of publication of this article were defrayed in part by the payment of page charges. This article must therefore be hereby marked *advertisement* in accordance with 18 U.S.C. Section 1734 solely to indicate this fact.

Received August 6, 2015; revised September 13, 2016; accepted October 10, 2016; published OnlineFirst October 31, 2016.

References

1. Bianchi M, Gandaglia G, Trinh QD, Hansen J, Becker A, Abdollah F, et al. A population-based competing-risks analysis of survival after nephrectomy for renal cell carcinoma. Urol Oncol 2014;32:46.e1–7.
2. Hutson TE, Bukowski RM, Cowey CL, Figlin R, Escudier B, Sternberg CN. Sequential use of targeted agents in the treatment of renal cell carcinoma. Crit Rev Oncol Hematol 2011;77:48–62.
3. Schatton T, Frank MH. Antitumor immunity and cancer stem cells. Ann N Y Acad Sci 2009;1176:154–69.
4. Topfer K, Kempe S, Muller N, Schmitz M, Bachmann M, Cartellieri M, et al. Tumor evasion from T cell surveillance. J Biomed Biotechnol 2011;2011: 918471.
5. Wilkie KP, Hahnfeldt P. Tumor-immune dynamics regulated in the microenvironment inform the transient nature of immune-induced tumor dormancy. Cancer Res 2013;73:3534–44.
6. Pardoll DM.The blockade of immune checkpoints in cancer immunotherapy. Nat Rev Cancer 2012;12:252–64.
7. Gabrilovich DI, Nagaraj S. Myeloid-derived suppressor cells as regulators of the immune system. Nat Rev Immunol 2009;9:162–74.
8. Ostrand-Rosenberg S.Myeloid-derived suppressor cells: more mechanisms for inhibiting antitumor immunity. Cancer Immunol Immunother 2010; 59:1593–600.
9. Najjar YG, Finke JH. Clinical perspectives on targeting of myeloid derived suppressor cells in the treatment of cancer. Front Oncol 2013;3:49.
10. Rodriguez PC, Hernandez CP, Quiceno D, Dubinett SM, Zabaleta J, Ochoa JB, et al. Arginase I in myeloid suppressor cells is induced by COX-2 in lung carcinoma. J Exp Med 2005;202:931–9.
11. Serafini P, Mgebroff S, Noonan K, Borrello I. Myeloid-derived suppressor cells promote cross-tolerance in B-cell lymphoma by expanding regulatory T cells. Cancer Res 2008;68:5439–49.
12. Sinha P, Clements VK, Ostrand-Rosenberg S. Interleukin-13-regulated M2 macrophages in combination with myeloid suppressor cells block immune surveillance against metastasis. Cancer Res 2005;65:11743–51.
13. Kujawski M, Kortylewski M, Lee H, Herrmann A, Kay H, Yu H. Stat3 mediates myeloid cell-dependent tumor angiogenesis in mice. J Clin Invest 2008;118:3367–77.
14. Yang L, DeBusk LM, Fukuda K, Fingleton B, Green-Jarvis B, Shyr Y, et al. Expansion of myeloid immune suppressor Gr+CD11b+ cells in tumor-bearing host directly promotes tumor angiogenesis. Cancer Cell 2004;6: 409–21.
15. Gabrilovich DI, Ostrand-Rosenberg S, Bronte V. Coordinated regulation of myeloid cells by tumours. Nat Rev Immunol 2012;12:253–68.
16. Diaz-Montero CM, Salem ML, Nishimura MI, Garrett-Mayer E, Cole DJ, Montero AJ. Increased circulating myeloid-derived suppressor cells correlate with clinical cancer stage, metastatic tumor burden, and doxorubicin-cyclophosphamide chemotherapy. Cancer Immunol Immunother 2009; 58:49–59.
17. Ko JS, Rayman P, Ireland J, Swaidani S, Li G, Bunting KD, et al. Direct and differential suppression of myeloid-derived suppressor cell subsets by sunitinib is compartmentally constrained. Cancer Res 2010;70: 3526–36.
18. Zea AH, Rodriguez PC, Atkins MB, Hernandez C, Signoretti S, Zabaleta J, et al. Arginase-producing myeloid suppressor cells in renal cell carcinoma patients: a mechanism of tumor evasion. Cancer Res 2005;65: 3044–8.
19. Walter S, Weinschenk T, Stenzl A, Zdrojowy R, Pluzanska A, Szczylik C, et al. Multipeptide immune response to cancer vaccine IMA901 after single-dose cyclophosphamide associates with longer patient survival. Nat Med 2012; 18:1254–61.
20. Diaz-Montero CM, Finke J, Montero AJ. Myeloid-derived suppressor cells in cancer: therapeutic, predictive, and prognostic implications. Semin Oncol 2014;41:174–84.
21. Solito S, Falisi E, Diaz-Montero CM, Doni A, Pinton L, Rosato A, et al. A human promyelocytic-like population is responsible for the immune suppression mediated by myeloid-derived suppressor cells. Blood 2011; 118:2254–65.
22. Gabitass RF, Annels NE, Stocken DD, Pandha HA, Middleton GW. Elevated myeloid-derived suppressor cells in pancreatic, esophageal and gastric cancer are an independent prognostic factor and are associated with significant elevation of the Th2 cytokine interleukin-13. Cancer Immunol Immunother 2011;60:1419–30.
23. Arihara F, Mizukoshi E, Kitahara M, Takata Y, Arai K, Yamashita T, et al. Increase in CD14+HLA-DR -/low myeloid-derived suppressor cells in hepatocellular carcinoma patients and its impact on prognosis. Cancer Immunol Immunother 2013;62:1421–30.
24. Huang A, Zhang B, Wang B, Zhang F, Fan KX, Guo YJ. Increased CD14(+) HLA-DR (-/low) myeloid-derived suppressor cells correlate with extrathoracic metastasis and poor response to chemotherapy in non-small cell lung cancer patients. Cancer Immunol Immunother 2013;62:1439–51.
25. Serafini P, De Santo C, Marigo I, Cingarlini S, Dolcetti L, Gallina G, et al. Derangement of immune responses by myeloid suppressor cells. Cancer Immunol Immunother 2004;53:64–72.
26. Movahedi K, Guilliams M, Van den Bossche J, Van den Bergh R, Gysemans C, Beschin A, et al. Identification of discrete tumor-induced myeloid-derived suppressor cell subpopulations with distinct T cell-suppressive activity. Blood 2008;111:4233–44.
27. Nagaraj S, Gupta K, Pisarev V, Kinarsky L, Sherman S, Kang L, et al. Altered recognition of antigen is a mechanism of CD8+ T cell tolerance in cancer. Nat Med 2007;13:828–35.

28. Raychaudhuri B, Rayman P, Ireland J, Ko J, Rini B, Borden EC, et al. Myeloid-derived suppressor cell accumulation and function in patients with newly diagnosed glioblastoma. Neuro Oncol 2011;13:591–9.
29. Obermajer N, Muthuswamy R, Odunsi K, Edwards RP, Kalinski P. PGE(2)-induced CXCL12 production and CXCR4 expression controls the accumulation of human MDSCs in ovarian cancer environment. Cancer Res 2011;71:7463–70.
30. Cacalano G, Lee J, Kikly K, Ryan AM, Pitts-Meek S, Hultgren B, et al. Neutrophil and B cell expansion in mice that lack the murine IL-8 receptor homolog. Science 1994;265:682–4.
31. Rot A, von Andrian UH. Chemokines in innate and adaptive host defense: basic chemokinese grammar for immune cells. Annu Rev Immunol 2004; 22:891–928.
32. Highfill SL, Cui Y, Giles AJ, Smith JP, Zhang H, Morse E, et al. Disruption of CXCR2-mediated MDSC tumor trafficking enhances anti-PD1 efficacy. Sci Transl Med 2014;6:237ra67.
33. Wolpe SD, Cerami A. Macrophage inflammatory proteins 1 and 2: members of a novel superfamily of cytokines. FASEB J 1989;3:2565–73.
34. Wolpe SD, Davatelis G, Sherry B, Beutler B, Hesse DG, Nguyen HT, et al. Macrophages secrete a novel heparin-binding protein with inflammatory and neutrophil chemokinetic properties. J Exp Med 1988;167:570–81.
35. Hirose K, Hakozaki M, Nyunoya Y, Kobayashi Y, Matsushita K, Takenouchi T, et al. Chemokine gene transfection into tumour cells reduced tumorigenicity in nude mice in association with neutrophilic infiltration. Br J Cancer 1995;72:708–14.
36. Rodriguez PC, Ernstoff MS, Hernandez C, Atkins M, Zabaleta J, Sierra R, et al. Arginase I-producing myeloid-derived suppressor cells in renal cell carcinoma are a subpopulation of activated granulocytes. Cancer Res 2009;69:1553–60.
37. Trellakis S, Bruderek K, Hutte J, Elian M, Hoffmann TK, Lang S, et al. Granulocytic myeloid-derived suppressor cells are cryosensitive and their frequency does not correlate with serum concentrations of colony-stimulating factors in head and neck cancer. Innate Immun 2013;19:328–36.
38. Jamieson T, Clarke M, Steele CW, Samuel MS, Neumann J, Jung A, et al. Inhibition of CXCR2 profoundly suppresses inflammation-driven and spontaneous tumorigenesis. J Clin Invest 2012;122:3127–44.
39. Katoh H, Wang D, Daikoku T, Sun H, Dey SK, Dubois RN. CXCR2-expressing myeloid-derived suppressor cells are essential to promote colitis-associated tumorigenesis. Cancer Cell 2013;24:631–44.
40. Yang L, Huang J, Ren X, Gorska AE, Chytil A, Aakre M, et al. Abrogation of TGF beta signaling in mammary carcinomas recruits Gr-1+CD11b+ myeloid cells that promote metastasis. Cancer Cell 2008;13:23–35.
41. Fan Q, Gu D, Liu H, Yang L, Zhang X, Yoder MC, et al. Defective TGF-beta signaling in bone marrow-derived cells prevents hedgehog-induced skin tumors. Cancer Res 2014;74:471–83.
42. Bunt SK, Sinha P, Clements VK, Leips J, Ostrand-Rosenberg S. Inflammation induces myeloid-derived suppressor cells that facilitate tumor progression. J Immunol 2006;176:284–90.
43. Charo IF, Ransohoff RM. The many roles of chemokines and chemokine receptors in inflammation. N Engl J Med 2006;354:610–21.
44. Chang MS, McNinch J, Basu R, Simonet S. Cloning and characterization of the human neutrophil-activating peptide (ENA-78) gene. J Biol Chem 1994;269:25277–82.
45. Dinarello CA.Biologic basis for interleukin-1 in disease. Blood 1996;87: 2095–147.
46. Youn JI, Kumar V, Collazo M, Nefedova Y, Condamine T, Cheng P, et al. Epigenetic silencing of retinoblastoma gene regulates pathologic differentiation of myeloid cells in cancer. Nat Immunol 2013;14:211–20.
47. Corzo CA, Condamine T, Lu L, Cotter MJ, Youn JI, Cheng P, et al. HIF-1alpha regulates function and differentiation of myeloid-derived suppressor cells in the tumor microenvironment. J Exp Med 2010;207: 2439–53.
48. Cui TX, Kryczek I, Zhao L, Zhao E, Kuick R, Roh MH, et al. Myeloid-derived suppressor cells enhance stemness of cancer cells by inducing microRNA101 and suppressing the corepressor CtBP2. Immunity 2013;39: 611–21.
49. Ko JS, Zea AH, Rini BI, Ireland JL, Elson P, Cohen P, et al. Sunitinib mediates reversal of myeloid-derived suppressor cell accumulation in renal cell carcinoma patients. Clin Cancer Res 2009;15:2148–57.
50. Appay V, Rowland-Jones SL. RANTES: a versatile and controversial chemokine. Trends Immunol 2001;22:83–7.
51. Asfaha S, Dubeykovskiy AN, Tomita H, Yang X, Stokes S, Shibata W, et al. Mice that express human interleukin-8 have increased mobilization of immature myeloid cells, which exacerbates inflammation and accelerates colon carcinogenesis. Gastroenterology 2013;144:155–66.
52. Waugh DJ, Wilson C. The interleukin-8 pathway in cancer. Clin Cancer Res 2008;14:6735–41.
53. Konig B, Steinbach F, Janocha B, Drynda A, Stumm M, Philipp C, et al. The differential expression of proinflammatory cytokines IL-6, IL-8 and TNF-alpha in renal cell carcinoma. Anticancer Res 1999;19:1519–24.
54. Harmon CS, DePrimo SE, Figlin RA, Hudes GR, Hutson TE, Michaelson MD, et al. Circulating proteins as potential biomarkers of sunitinib and interferon-alpha efficacy in treatment-naive patients with metastatic renal cell carcinoma. Cancer Chemother Pharmacol 2014;73:151–61.
55. Kowalczuk O, Burzykowski T, Niklinska WE, Kozlowski M, Chyczewski L, Niklinski J. CXCL5 as a potential novel prognostic factor in early stage non-small cell lung cancer: results of a study of expression levels of 23 genes. Tumour Biol 2014;35:4619–28.
56. Polimeno M, Napolitano M, Costantini S, Portella L, Esposito A, Capone F, et al. Regulatory T cells, interleukin (IL)-6, IL-8, vascular endothelial growth factor (VEGF), CXCL10, CXCL11, epidermal growth factor (EGF) and hepatocyte growth factor (HGF) as surrogate markers of host immunity in patients with renal cell carcinoma. BJU Int 2013;112:686–96.
57. Wald G, Barnes KT, Bing MT, Kresowik TP, Tomanek-Chalkley A, Kucaba TA, et al. Minimal changes in the systemic immune response after nephrectomy of localized renal masses. Urol Oncol 2014;32:589–600.
58. Tran HT, Liu Y, Zurita AJ, Lin Y, Baker-Neblett KL, Martin AM, et al. Prognostic or predictive plasma cytokines and angiogenic factors for patients treated with pazopanib for metastatic renal-cell cancer: a retrospective analysis of phase 2 and phase 3 trials. Lancet Oncol 2012;13:827–37.
59. Gahan JC, Gosalbez M, Yates T, Young EE, Escudero DO, Chi A, et al. Chemokine and chemokine receptor expression in kidney tumors: molecular profiling of histological subtypes and association with metastasis. J Urol 2012;187:827–33.
60. Philips GK, Atkins MB. New agents and new targets for renal cell carcinoma. Am Soc Clin Oncol Educ Book 2014:e222–7.
61. Xu L, Zhu Y, An H, Liu Y, Lin Z, Wang G, et al. Clinical significance of tumor-derived IL-1beta and IL-18 in localized renal cell carcinoma: associations with recurrence and survival. Urol Oncol 2015;33:68.e9–16.